Variation of molecular ions in the inner magnetosphere observed by the Arase satellite

A. Nagatani[1], Y. Miyoshi[1], K. Asamura[2], L. M. Kistler[1,3], S. Nakamura[1], K. Seki[4], Y. Ogawa[5] , and I. Shinohara[2]

[1] Institute for Space-Earth Environmental Research, Nagoya University, Nagoya, Japan

[2] JAXA, Sagamihara, Japan

[3] University of New Hampshire, Durham, NH, US.

[4] University of Tokyo, Tokyo, Japan

[5] National Institute for Polar Research, Tachikawa, Japan

Corresponding author: Yoshizumi Miyoshi (miyoshi@isee.nagoya-u.ac.jp)

Key Points:

- Systematic molecular ion observations in the inner magnetosphere for 6.5 years.

- Molecular ion counts increase following enhancements in the solar wind dynamic pressure.

- The ratio of molecular ions to O^+ was lower in the rising phase of the solar cycle than that during the solar minimum.

Abstract

We analyzed time-of-flight (TOF) data from the Arase satellite to investigate temporal variations of O_2^+, NO^+, and N_2^+ at 19.2 keV/q in the inner magnetosphere for 6.5 years from the solar declining to rising phases. Molecular ion counts were estimated by subtracting the background contamination of oxygen counts. While the number of clear molecular events was small, the estimated molecular ion counts exhibited good correlation with the solar wind dynamic pressure and SYM-H index. Long-term variations of molecular ions were different from that of oxygen ions. Additionally, we discuss the importance of the solar wind dynamic pressure in causing the escape of molecular ions into the magnetosphere through an increase in the convection electric field, which causes different evolutions of oxygen ions and molecular ions.

Plain language summary

Molecular ions (O_2^+, NO^+, and N_2^+) have been observed in the magnetosphere. Molecular ions in the ionosphere are required to obtain energy through short-lived reactions with electrons to escape from low altitudes at the ionosphere to the magnetosphere. The escaping mechanisms of molecular ions are not fully understood. This study analyzed 6.5 years of data from the Arase satellite to investigate long-term variations of molecular ions in the inner magnetosphere. We developed a reliable dataset of the molecular ions from the TOF observations. Our results suggest solar wind dynamic pressure increases can enhance molecular ions escape from the ionosphere into the magnetosphere through the increase of the convection electric fields.

1 Introduction

[1]

Heavy ions with single charge states, such as O^+ and N^+, and molecular ions such as O_2^+, NO^+, and N_2^+, originate from the Earth's ionosphere, and are transported to the magnetosphere. The outflow of O+ ions has been the subject of numerous studies (e.g., Yau et al., 2007; Glocer et al., 2012; Keika et al., 2013; Ilie et al., 2015), and escape mechanisms that involve photoionization, electron precipitation, ion-electron-neutral chemistry, and collisions, have been considered. Compared to atomic ions, molecular ions peak at much lower altitudes, ~150-200 km, and therefore are required to obtain energy in short dissociative recombination lifetimes with electrons to escape from low altitudes; however, the molecular ion outflow mechanisms are not well known (Lin and Ilie, 2022).

[2]

Molecular ions in the magnetosphere were first reported using the DE-1 satellite (Craven et al., 1985). The DE-1 satellite observations suggest that molecular ions are produced in the polar cusp region, and transported to the nightside and polar cap by convection electric fields. The Polar satellite observed molecular ions and found that their detection was more sensitive to enhanced geomagnetic conditions than that for O^+ detection (Lennartsson et al., 2000). They suggested that the pathway and energization mechanisms of molecular ions are distinct from those of O^+, because molecular ions appear to be more enhanced during geomagnetic activity. Recently, Takada et al. (2021) investigated the upflows of molecular ions in the thermosphere using EISCAT radar observations, and showed a significant outflow of molecular ions during coronal mass ejection (CME)- and corotating interaction region (CIR) driven storms.

61   [3]

62   The AMPTE satellite revealed the presence of molecular NO^+ and O_2^+ ions at $L \sim 6.5$–7 in the
63   equatorial magnetosphere with energies of approximately 100 keV/q during storms, while there
64   were no molecular ion events during geomagnetically quiet times (Klecker et al., 1986). The
65   AMPTE observations also showed that molecular ions were detected a few to 16 h after sudden
66   storm commencement (SSC). These molecular ions contributed ~0.5% of the total energy of 32
67   keV/cm^{-3} in the energy range of 20–230 keV/q (Klecker et al., 1986). The presence of these
68   energetic molecular ions suggests that their efficient heating during transport from the
69   ionosphere to the magnetosphere is influenced by mass-dependent energization mechanisms or
70   the density profile of the thermosphere during storms. Model calculations (Sojka and Schunk,
71   1984) have shown that the densities of molecular ions above ~ 300 km increase by several orders
72   of magnitude during the main phase of a magnetic storm. Data observed by Geotail/STICS in the
73   magnetotail over 20 years (1995-2015) showed that the molecular ion count rates of
74   magnetospheric molecular ions have a strong response to geomagnetic activity. Moreover,
75   molecular ions and atomic N^+ and O^+ ions react differently to the solar F10.7 flux (Christon et
76   al., 2020).

77

78   [4]

79   Lin and Ilie (2022) reviewed the past observations of magnetospheric molecular ions and
80   concluded that the probability of observing molecular ions in the magnetosphere during quiet
81   periods was nearly negligible. Recently, the Arase satellite has observed molecular ions more
82   frequently in the inner magnetosphere. Using Arase satellite data, Seki et al. (2019) reported that
83   molecular ions are frequently observed at L=2.5-6.6 during storms. The frequent appearance of
84   molecular ions in the inner magnetosphere suggests a higher occurrence of molecular ion
85   outflows during storm periods than previously estimated, as earlier studies presumed that
86   molecular ions were only detectable during severe storms (Dst $\leq$ -100 nT). These results suggest
87   that magnetic storms are not always necessary for molecular ion enhancement, and systematic
88   observations of molecular ions are necessary to reveal the occurrence of molecular ions in the
89   inner magnetosphere. In this study, we analyze systematic molecular ion observation data
90   obtained by the Arase satellite since April, 2017 during the late declining phase of the solar cycle
91   24 and early rising phase of the solar cycle 25. This period covers quiet geomagnetic conditions,
92   as well as several severe magnetic storms. Using Arase time-of-flight (TOF) data, we
93   investigated long-term variations in molecular ions and their dependence on geomagnetic
94   activity and solar wind parameters.

95   **2 Analysis of the Arase TOF data**

96   [5]

97   In this study, we used data from the LEPi instrument (Asamura et al., 2018) onboard the Arase
98   satellite (Miyoshi et al., 2018), which covers energies from 0.01 to 25 keV/q. LEPi uses TOF
99   method to measure the flight time of incoming ions inside a sensor to differentiate ion species.
100   LEPi has two observation modes: normal and TOF. In the normal mode, LEPi provides ion
101   fluxes as a function of energy, incoming direction, and ion species estimated by the measured
102   particle TOF. In the TOF mode, the ion fluxes are provided as a function of the measured

103 particle TOF rather than the estimated species, allowing minor ions to be observed. The TOF
104 mode is typically used during the outbound pass of every fourth orbit.

105 [6]

106 **Figure 1(a) and (b)**show energy spectra of H^+ and O^+ count rates observed in the TOF mode
107 from 15:16 to 19:50 UT on May 28, 2017. During this time period, the satellite traversed from
108 *L*=2.5 to 6.0 on the morning side under the early phase of recovery following a storm on May 28.
109 Enhancements in the H^+ and O^+ ion count rates associated with storms are particularly noticeable
110 after 16:30. **Figure 1(c)** shows the accumulated counts as a function of TOF (measured flight
111 time) and energy during this time period. The TOF depends on both the mass and energy of each
112 ion species. Although LEPi detected multiple ion species in the inner magnetosphere, there are
113 fewer counts at low energies, and the peaks are closely spaced at higher energies, making it more
114 difficult to distinguish the individual peaks. Therefore, we focused on the data obtained at 19. 2
115 keV/q, since significant counts and clear peaks depending on ion species are obtained. **Figure
116 1(d)** shows the TOF profile at an energy of 19.2 keV/q (black lines). A tail of the ion peaks
117 toward longer TOF in **Figure 1(d)** is due to energy loss and angular straggling of incoming ions
118 passing through the ultra-thin carbon foil installed in the instrument. The tail of O^+ TOF profile
119 overlaps to the TOF profile of molecular ions, where the accumulated count of molecular ions
120 (highlighted in purple) is approximately two orders of magnitude smaller than that of O^+
121 (highlighted in yellow). It is necessary to remove this O^+ tail influence to accurately determine
122 the molecular ion count.

123

124 [7]

125 To estimate the actual molecular ion counts for LEPi TOF, it is important to estimate the
126 background counts, including the O^+ ion counts and ambient noise. Several methods have been
127 developed for deriving ion counts from TOF observations of the satellites. Seki et al. (2019)
128 applied Gaussian function fitting to derive molecular ions for the Arase/MEPi observations.
129 Mouikis et al. (2014) applied a subtraction method to estimate the background noise for the
130 Cluster/CODIF observations. Since the molecular ion counts detected by LEPi were too small to
131 estimate with fitting, we constructed "a reference profile" to model the O^+ TOF profile, as shown
132 by the red line in **Figure 1(d)**. First, for each TOF spectrum, count averaged over 312 to 390 ns,
133 where there are no significant TOF profiles of major ion species, was subtracted from all the
134 TOF bins, since the noise source such as penetrating radiations appears as constant counts over
135 the TOF spectrum. Then, to define the reference profile, we selected the TOF spectrum on March
136 15, 2023 as the reference in which the O^+ TOF profile was well identified without any significant
137 counts of molecular ions. To obtain the smooth reference profile, we performed a quadratic least
138 squares fit to the reference TOF profile ranging from 60 to 86 ns which covers the major part of
139 the TOF spectrum of molecular ions. Then the reference profile was normalized to the O^+ peak
140 count of each observation. Molecular ion count was obtained by subtracting the reference profile
141 from the observed TOF spectrum and summed over the TOF range of molecular ions (purple). In
142 case of **Figure 1(d)**, the counts of H^+ and O^+ are 4.5 x 10^6 and 3.9 x 10^6 that are estimated from
143 the same fitting method as Funsten et al. (2013), while the count of molecular ions estimated
144 from this method is 8.2 x 10^3, which is small compared to those for H^+ and O^+. After visual

145 inspection of all the Arase TOF data for 6.5 years from April 2017 to December 2023, the count
146 data without a significant peak for molecular ions were eliminated from the further analysis in
147 this study.

148

149 **3 Results**

150 [8]

151 **Figure 2** shows molecular ion counts observed in two distinct events. The panels show the
152 molecular ion counts, *L*-value where Arase was located, IMF Bz, solar wind speed, solar wind
153 dynamic pressure, SYM-H index, and SML index on July 19, 2019 (**Figure 2(a)**) and March 14,
154 2022 (**Figure 2(b)**). Molecular ion counts were estimated by accumulating data over a 10-minute
155 period. Blue shaded areas indicate the time intervals of the TOF mode measurements using the
156 LEP-i instrument. As shown in Figure 2, these events are driven by CIR and CME (Miyoshi and
157 Kataoka, 2005).

158

159 [9]

160 The first event was caused by a CIR and subsequent coronal hole stream. The amplitude of the
161 minimum SYM-H index was -42 nT. Molecular ions were detected during the recovery phase,
162 and the maximum count was 947 at *L*=5.28 after the sudden commencement (SC) caused by an
163 enhancement in the solar wind dynamic pressure of up to 19.1 nPa. It is worth noting that
164 molecular ions were not found in the TOF observations at 3:28 – 7:45 on July 9, immediately
165 after the SC. This implies that ion transport from the ionosphere to the magnetosphere requires a
166 finite time. This observation shows that molecular ions associated with the solar wind dynamic
167 pressure enhancement can exist in the inner magnetosphere without severe magnetic storms.

168

169 [10]

170 The second event was driven by a CME. Sheath and magnetic clouds were observed, and the
171 minimum SYM-H index was – 114 nT. The maximum count was approximately 1344 at *L*=
172 4.18. The SC was observed in association with the enhancement of solar wind dynamic pressure
173 up to 17.7 nPa. Molecular ions were observed during the storm recovery phase. While the storm
174 amplitude and solar wind drivers were different from those of the first event, the SC caused by
175 solar wind dynamic pressure enhancement was commonly observed before the increase in the

176 molecular ion count in the inner magnetosphere. This is consistent with previous observations
177 (Klecker et al., 1986) that molecular ions are observed after SSC.

178

179
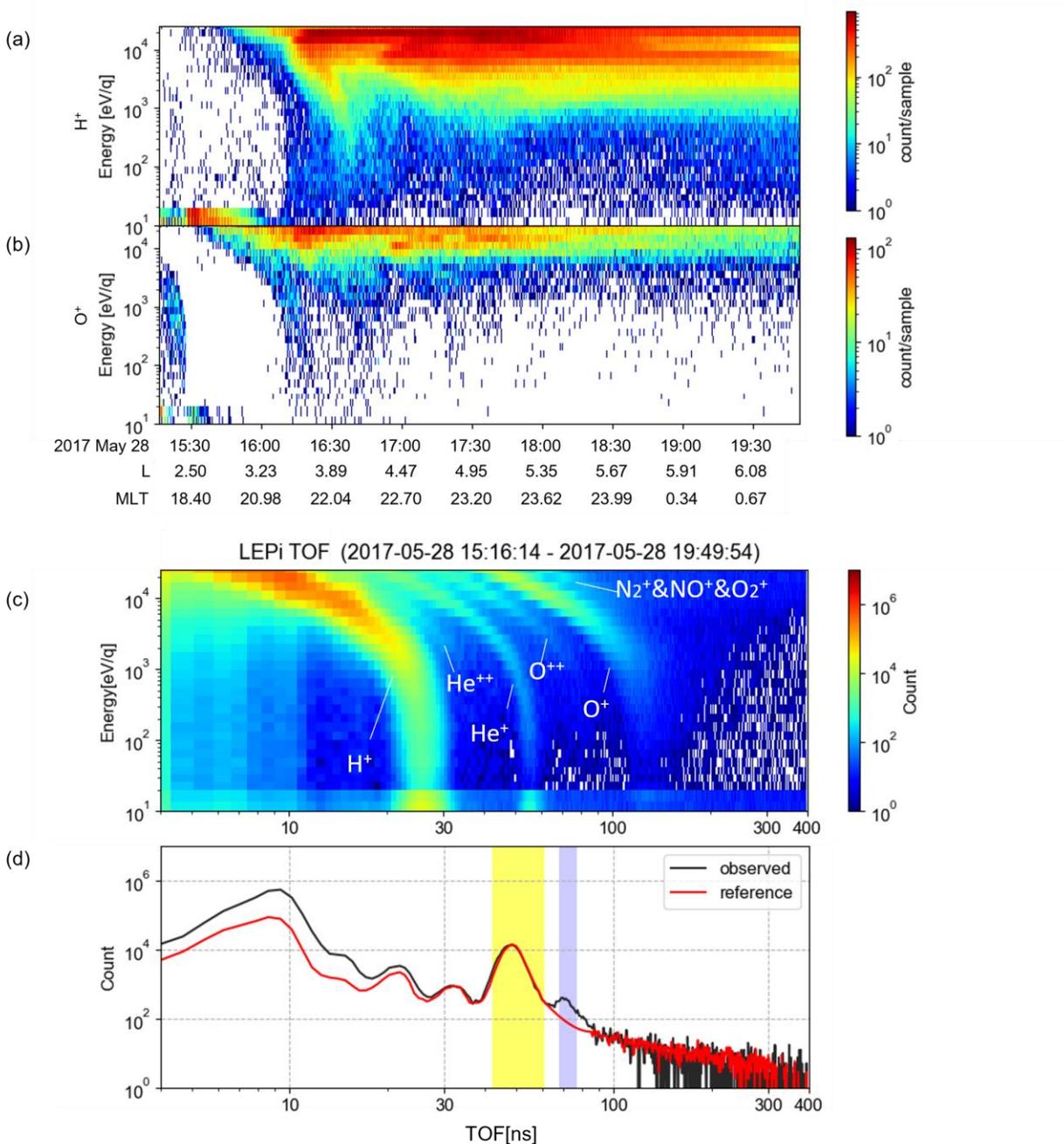
Figure 1. Time-energy diagram of **(a)** H^+ and **(b)** O^+ observed at 15:16-19:50 UT on May 28, 2017 for consideration of time variation of count rate change over pass. **(c)** TOF-energy diagram observed at the same time interval. The color indicates the counts of ions. **(d)** TOF spectrum on May 28, 2017 at 19.2 keV/q. Observed data (black line), reference profile (red line), TOF range

184 of O$^+$ (yellow shaded), and TOF range of molecular ions (purple shaded); **(c)** and **(d)** shows the
185 data summed within 1 outbound pass.
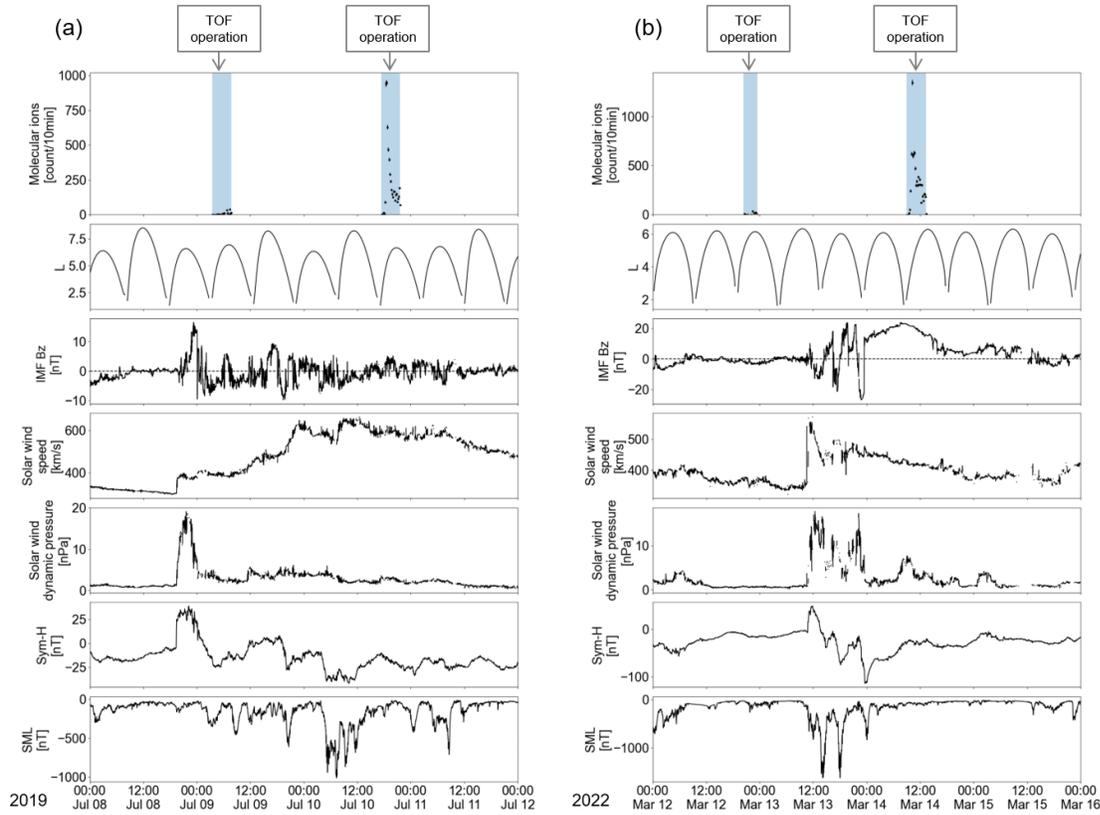
Figure 2

186

187

188 **Figure 2.** LEPi detected molecular ions events on **(a)** July 10, 2019, **(b)** March 14, 2022. From
189 top to bottom, molecular ion count, *L*-value of the Arase satellite, IMF Bz, solar wind velocity,
190 solar wind dynamic pressure, SYM-H, and SML index respectively. The blue shaded areas in the
191 top panels show the time intervals of TOF mode operation.

192

193 [11]

194 Next, we show the parameter dependence of the molecular ion counts. We found 14 clear
195 molecular ion events from Arase observations over 6.5 years. **Table S1** shows the 14 observed
196 events. 13 of the 14 events were associated with CIR or CME. As can be seen from the table, on
197 April 4 and 5, 2017 and May 28 and 29, 2017 molecular ions were observed in two consecutive
198 observation passes. For the correlation analysis hereafter, the molecular ion counts on April 4
199 and May 28 will be used as representatives for these events. **Figures 3 (a)**, **(b)**, and **(c)** show the
200 correlation between the molecular ion count and solar wind dynamic pressure, SYM-H index,

201   and SML index for these events. The parameter used for this correlation study was the maximum
202   absolute value of the parameter within two days before molecular ion detection. The molecular
203   ion count increased with the solar wind dynamic pressure, and increased twofold when the solar
204   wind dynamic pressure increased by a factor of 1.5. The correlation coefficient between the
205   molecular ion count and solar wind dynamic pressure was 0.68. In all events, solar wind dynamic
206   pressure enhancement occurred before the observation of the molecular ions. The correlation
207   with the SYM-H index was also significant; the molecular ion count increased at the same rate as
208   that for the SYM-H index; the correlation coefficient was -0.75. It is important to note that the
209   minimum SYM-H of the six events is higher (less negative) than -50 nT, indicating that
210   molecular ions can exist in the inner magnetosphere during non-storm times if there is a solar
211   wind dynamic pressure enhancement. The molecular ion counts showed a good correlation with
212   the SML index, with a correlation coefficient of -0.70. Note that the SML index has not been
213   available for the September 18, 2023 event, the correlation coefficient is estimated from other 13
214   events. It was found that there is a relationship between magnetospheric molecular ion counts

215 and the intensity of substorms. We also investigated the correlations between the solar wind
216 velocity; however, the correlation coefficient was lower than 0.5.

217
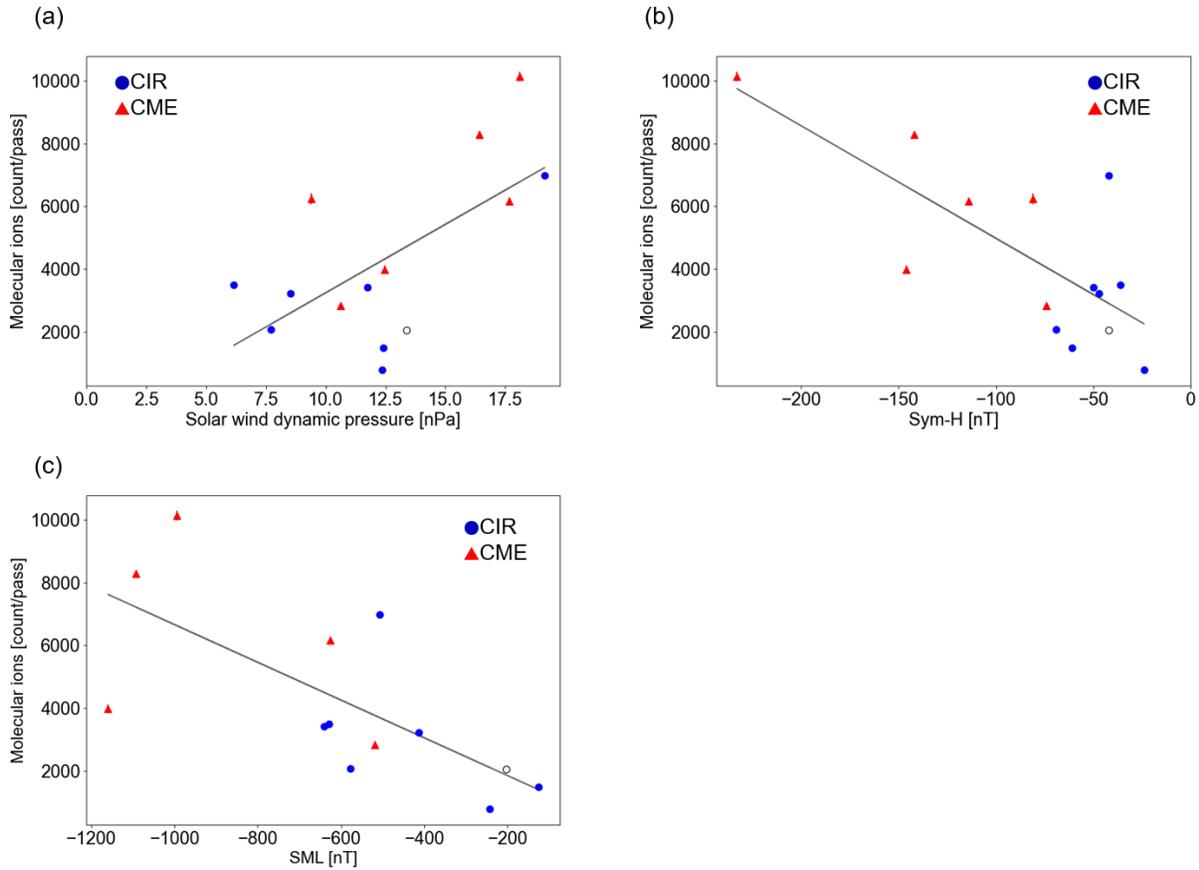
218

219

220 **Figure 3.** Relationship between the molecular ion counts and **(a)** solar wind dynamic pressure,
221 **(b)** SYM-H index, and **(c)** SML index. Blue dots are related to CIR and red triangles are related
222 to CME.

223 [12]

224 To obtain sufficient counts of molecular ions, we integrated the TOF profile data for six months.
225 When a clear peak for the molecular ions was observed, we derived the molecular ion counts
226 using the same method as that in the previous analysis. The peak of the molecular ions in the
227 TOF profile was not clear after the second half of 2021, probably owing to enhancements in

228   oxygen ions. The red dots in **Figure 4(b)** after the end of 2021 represent the cases in which there
229   were no significant molecular ion peaks in the TOF profiles (red circles).

230

231   [13]

232   **Figure 4** shows the time variations of the molecular ion counts, oxygen ion counts, and ratio of
233   molecular ions to oxygen ion counts. **Figure 4(a)** shows the long-term variations in the oxygen
234   ion counts. The variation in oxygen ion counts seems to correlate with solar activity. When
235   Arase observations began in 2017, counts were on the order of 5×10^4, falling to approximately
236   one-fifth of that by the first half of 2020. Thereafter, as the solar activity increased, the counts
237   increased to 2×10^6 in early 2023. **Figure 4(b)** shows the long-term variations in molecular ion
238   counts (N_2^+, NO^+, and O_2^+). In contrast to the oxygen ions, the molecular ions showed count
239   enhancements in early 2017, late 2019, and early 2021, with the variability unrelated to the solar
240   activity. Note that the data shown in red beyond the latter half of 2021 indicates that the
241   molecular ion peak was not clearly observed.

242   [14]

243   **Figure 4(c)** shows the ratio of the molecular ion count to the oxygen ion count. The ratio peaks
244   during the solar minimum, in contrast to the oxygen profile. If the same process contributes to
245   the escape of both molecular and oxygen ions, they should exhibit the same systematic
246   variations. These results suggest that different processes are responsible for the outflow of these
247   ionic species. Note that the molecular ion peak in the TOF spectrum disappears when the ratio

248   drops below ~1.5×10^{-3}, and thus, the upper limit is below the ratio measured during other time
249   periods shown in black circles.
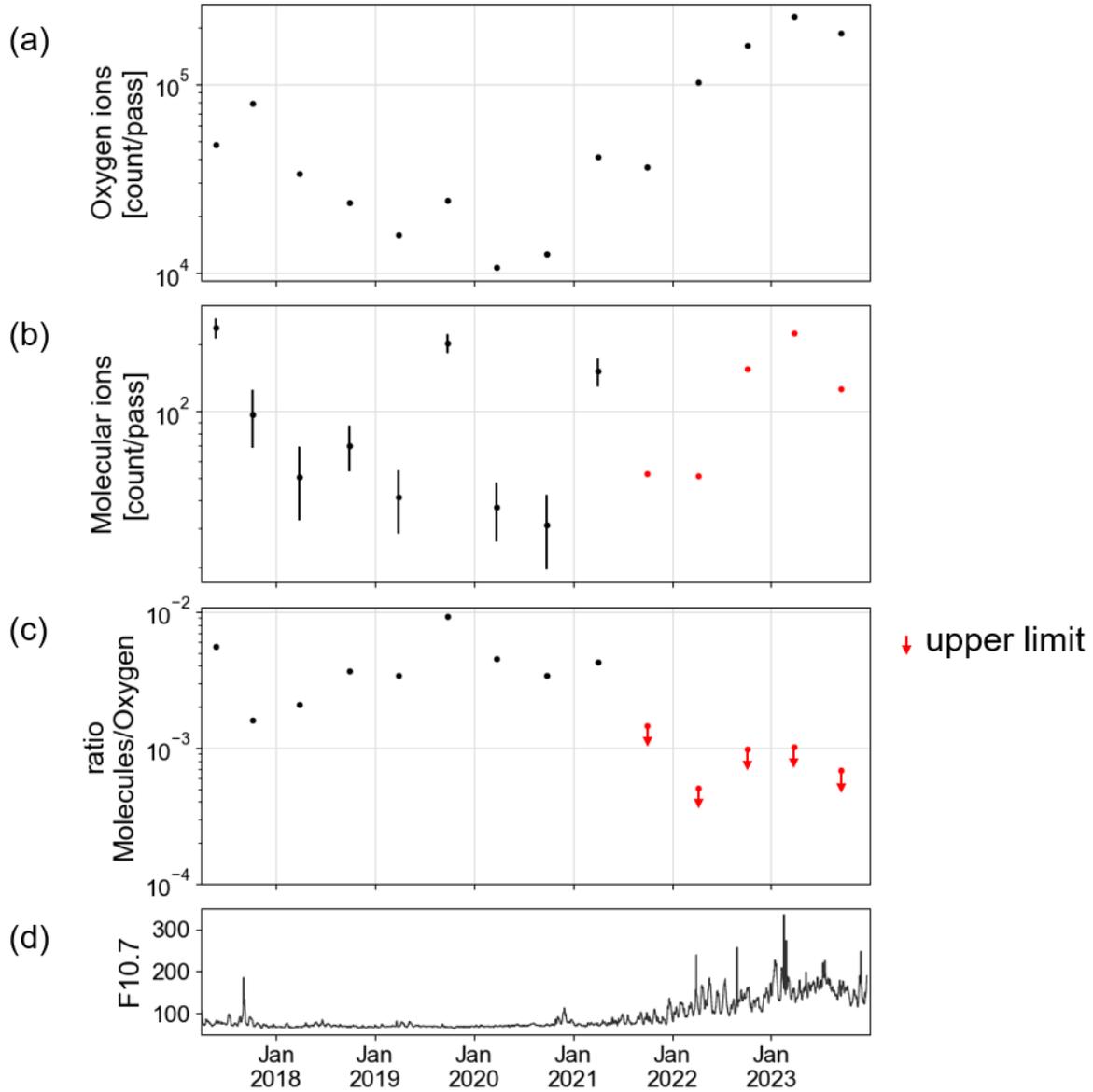
250

251   **Figure 4 (a)** Oxygen ion count, **(b)** molecular ion count, **(c)** ratio of molecular ion count to
252   oxygen ion count with the data summed and averaged over half a year. **(d)** The bottom panel
253   shows the F10.7 flux. The red circles in **(b)** correspond to the cases in which there were no

254 significant molecular ion peaks in the TOF profiles. The downward arrow in **(c)** indicates the
255 upper limit.

256

257 **4 Summary and Discussions**

258 [15]

259 In this study, we investigated the molecular ions in the inner magnetosphere observed by the
260 Arase satellite, which is the first observation of long-term variations in molecular ions in the
261 inner magnetosphere. To quantitatively investigate the molecular ions, we developed a method to
262 estimate the molecular ion counts from the TOF data. This method effectively eliminated the
263 influence of the O^+ TOF profile on the molecular ion TOF range and yielded a reliable dataset.
264 The estimated molecular ion counts showed good correlations with the solar wind dynamic
265 pressure, SYM-H index, and SML index.

266 [16]

267 Previous studies have suggested that molecular ions in the inner magnetosphere are observed
268 during large geomagnetic storms (Craven et al., 1985, Klecker et al., 1986), because a strong
269 energy input is necessary for molecular ions to escape from the upper atmosphere. Seki et al.
270 (2019) showed that energetic molecular ions are observed during small magnetic storms (Dst ~-
271 20 nT) from the Arase observations in 2017. As shown in **Figure 3(b)**, molecular ions can be
272 observed even during non-storm times (SYM-H > -30 nT) under significant enhancement of
273 solar wind dynamic pressure.

274

275   [17]

276 Schunk et al. (1975) show that owing to the rapid increase of the reaction $O^+ + N_2 \rightarrow NO^+ + N$
277 with ion energy, high-latitude electric fields deplete O^+ in favor of NO^+ after the increase of the
278 scale height of N_2. For large electric fields (~200 mV m^{-1}), NO^+ completely dominates the ion
279 composition up to at least 600-km altitudes. This reaction leads to a reduction in O^+ and
280 enhancement in NO^+ during periods of intense convection velocity. Wilson and Craven (1999)
281 demonstrated that the outflow of molecular ions necessitates specific conditions based on the
282 DE-1 observations, one of which is the presence of strong convection electric fields in the
283 ionosphere.

284

285 [18]

286 It should be noted that all events in **Figure 3(a)** are associated with a solar wind dynamic
287 pressure enhancement of more than 5 nPa during both storm and non-storm intervals. As shown
288 in **Figure 2**, SSCs caused by solar wind dynamic pressure enhancement were detected in ~85%
289 of the molecular ion events. The results suggest that the energy input associated with the solar
290 wind dynamic pressure is essential for the outflow of molecular ions from the upper atmosphere

291 to the inner magnetosphere, as suggested by AMPTE observations（Klecker et al., 1986). Gillie
292 et al. (2012) indicated that ionospheric convection is enhanced in association with SSC. The
293 results of this study suggest that an increase in the solar wind dynamic pressure leading to SSC
294 or SC events results in an increase in the convection electric field, which facilitates the
295 production and outflow of molecular ions into the magnetosphere. Enhancements in convection
296 electric fields are also observed during storm times; therefore, it is natural to find a correlation
297 between the SYM-H index and molecular ion counts, as shown in **Figure 3(b)**.

298

299 [20]

300 **Figure 4** shows the long-term variations in the molecular and oxygen ions in the inner
301 magnetosphere, where no systematic variations in the molecular ion counts are observed. The
302 molecular ion to oxygen ratio is the inverse of the oxygen count profile, and a potential scenario
303 to explain the long-term variations is as follows: during periods of solar minimum when the scale
304 height of O^+ is reduced, the reaction responsible for converting O^+ to NO^+ in the presence of
305 strong convection (Schunk et al., 1975) has a significant impact on the resulting composition of
306 the outflow, as evidenced by Arase observations that indicate a noticeable increase in molecular
307 ions. By contrast, during the solar maximum, when the scale height of O^+ is higher, the outflow
308 of O^+ occurs more readily. Since the outflow of oxygen ions far exceeds that of molecular ions, it
309 is likely that the molecular ions/O^+ ratio remains too low to be detected even when the flux of the
310 molecular ion outflow increases. This result is consistent with the observations from Geotail, as
311 reported by Christon et al. (2020), indicating that atomic and molecular ions demonstrate
312 different responses to F10.7.
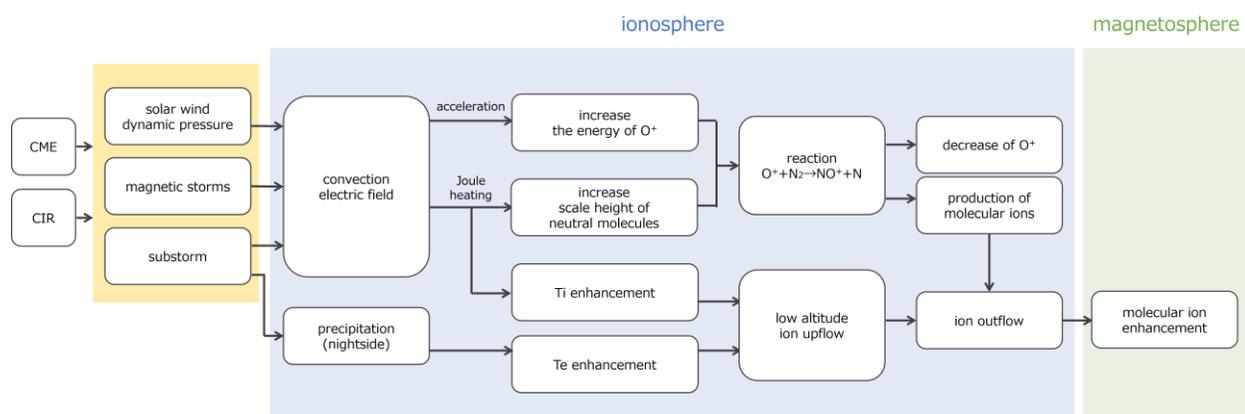
313

314 **Figure 5** Schematic diagram for the possible process leading to molecular ion outflow.

315

316 [21]

317 **Figure 5** shows a schematic diagram to summary the possible process based on these results. An
318 increase in solar wind dynamic pressure leads to an increase in the convection electric field. The
319 enhancement of the convection electric field influences the scale height of the neutral molecules
320 via the Joule heating and increases the energy of the oxygen ions. These processes lead to the

321   production of molecular ions by enhancing the reaction between oxygen ions and neutral
322   molecules. This reaction causes a decrease in O^+ and an increase in NO^+ (Schunk et al., 1975),
323   which is consistent with the results in **Figure 4**. As demonstrated by Takada et al.(2021), the ion
324   frictional heating resulting from the convection electric field triggers ion upflow in the
325   ionosphere. Taking this into account, it is conceivable that solar wind dynamic pressure
326   enhancement leads to ion upflow, which is comparatively rich in molecular ions. The observed
327   correlations between SYM-H and magnetospheric molecular ion counts (**Figure 3(b)**), as well as
328   the solar wind dynamic pressure and magnetospheric molecular ion counts (**Figure 3(a)**), are
329   consistent with this mechanism. It should be noted that the particle precipitation on the nightside
330   also causes the low-altitude ion upflow during CIR-driven magnetic storms and small CME-
331   driven storms (Takada, 2023). As shown in **Table S1**, our result shows that over 90% of the
332   events were observed associated with arrivals of CIR or CME in which an increase of
333   precipitation is expected. Therefore, it is suggested that particle precipitation in addition to the
334   enhancement of the convection electric field may also contributes to the enhancement of
335   molecular ions in the magnetosphere.

336   [22]

337   Considering the molecular ion upflow mechanisms, enhancement of convection electric fields is
338   essential. Solar wind dynamic pressure enhancement, magnetic storms, and substorms contribute
339   to the enhancement of the convection electric fields that drive the molecular ion upflow. As
340   shown in this study, molecular ions can exist in the inner magnetosphere associated with a
341   pressure enhancement even during non-storm periods. The oxygen and the molecular ions scale
342   heights depend on the solar cycle. Since the Arase observations in this study did not cover the
343   solar maximum, further observations of molecular ions in the inner magnetosphere are important
344   to clarify the outflow mechanism of molecular ions.

345

348   **Data Availability Statement**

349   The data for this study is archived in the ERG Science Center (ERG-SC) operated by
350   ISAS/JAXA and ISEE/Nagoya University (https://ergsc.isee.nagoya-u.ac.jp/index.shtml.en;
351   Miyoshi, Hori, et al., 2018). The present study used the Arase/LEPi data L2-v03 (Asamura,
352   Miyoshi and Shinohara, 2018, 10.34515/DATA.ERG-05001) and the Arase orbital data L2-v03
353   (Miyoshi, Shinohara, and Jun, 2018, 10.34515/DATA.ERG-12000) . The Sym-H index (WDC
354   Kyoto, 2022, 10.14989/267216) used in this paper/presentation was provided by the WDC for
355   Geomagnetism, Kyoto (http://wdc.kugi.kyoto-u.ac.jp/wdc/Sec3.html). The solar wind and IMF
356   data were obtained from NASA/GSFC's OMNI data set through the OMNIWeb
357   (https://omniweb.sci.gsfc.nasa.gov). The SML index is provided from SuperMAG
358   (http://supermag.jhuapl.edu/indices).

359   **References**

360 Asamura, K., Y. Kazama, S. Yokota, et al.(2018), Low-energy particle experiments–ion mass
361 analyzer (LEPi) onboard the ERG (Arase) satellite. *Earth Planets Space*, **70**, doi:
362 10.1186/s40623-018-0846-0

363 Asamura, K., Y. Miyoshi, and I. Shinohara(2018), The LEPi instrument Level-2 omniflux data
364 of Exploration of energization and Radiation in Geospace (ERG) Arase satellite,
365 doi:10.34515/DATA.ERG-05001.

366 Craven, P. D., R. C. Olsen, C. R. Chappell, and L. Kakani (1985). Observations of Molecular
367 Ions in the Earth's Magnetosphere. *J. Geophys. Res.*, **90**, 7599–7605.
368 doi:10.1029/JA090iA08p07599

369 Christon, S. P., D. C. Hamilton , D. G. Mitchell, J. M. C. Plane, and S. R. Nylund (2020).
370 Suprathermal magnetospheric atomic and molecular heavy ions at and near Earth, Jupiter, and

Saturn: Observations and identification. *J. Geophys. Res.*, **125**, e2019JA027271, doi:10.1029/2019JA027271

Funsten, H. O. et al. (2013), Helium, Oxygen, Proton and Electron (HOPE) mass spectrometer for the radiation belt storm probe mission, *Space Sci. Rev.*, **179**, 423-484, doi:10.1007/s11214-013-9968-7.

Gillies, D. M., J.-P. St.-Maurice, K. A. McWilliams, and S. Milan (2012), Global-scale observations of ionospheric convection variation in response to sudden increases in the solar wind dynamic pressure, *J. Geophys. Res.*, **117**, A04209, doi:10.1029/2011JA017255.

Glocer, A., N. Kitamura, G. Toth, and T. Gombosi (2012). Modeling solar zenith angle effects on the polar wind. *J. Geophys. Res*. **117**, A04318. doi:10.1029/2011JA017136

Ilie, R., M. W. Liemohn, G. Toth, N. Ganushkina, and L. K. S. Daldorff (2015). Assessing the role of oxygen on ring current formation and evolution through numerical experiments. *J. Geophys. Res. Space Phys*. **120**, 4656–4668. doi:10.1002/2015JA021157.2015JA021157

Keika, K., L. M. Kistler, and P. C. Brandt (2013). Energization of O^+ ions in the Earth's inner magnetosphere and the effects on ring current buildup: A review of previous observations and possible mechanisms. *J. Geophys. Res.*, **118**, 4441–4464.、 doi:10.1002/jgra.50371

Klecker, B., E. Möbius, D. Hovestadt, M. Scholer, G. Gloeckler, and F. M. Ipavich (1986). Discovery of energetic molecular ions (NO^+ and O_2^+) in the storm time ring current. *Geophys. Res. Lett.* **13**, 632–635. doi:10.1029/GL013i007p00632

Lennartsson, O.W., H.L. Collin, W.K. Peterson, and E.G. Shelley, (2000) Polar/TIMAS statistical results on the outflow of molecular ions from earth at solar minimum, *Adv. Space Res.*, **25**, doi:10.1016/S0273-1177(99)00531-1.

Lin M-Y and R. Ilie (2022) A Review of Observations of Molecular Ions in the Earth's Magnetosphere Ionosphere System. *Front. Astron. Space Sci*. 8:745357. doi: 10.3389/fspas.2021.74535

Miyoshi, Y., I. Shinohara, T. Takashima et al.(2018), Geospace exploration project ERG. *Earth Planets Space,* **70**, 101, doi:10.1186/s40623-018-0862-0

Miyoshi, Y., and R. Kataoka (2005), Ring current ions and radiation belt electrons during geomagnetic storms driven by coronal mass ejections and corotating interaction regions, *Geophys. Res. Lett.* **32**, L21105, doi:10.1029/2005GL024590.

Miyoshi, Y., T. Hori et al., (2018), The ERG Science Center, *Earth, Planets Space*, **70**, doi:10.1186/s40623-018-0867-8.

Miyoshi, Y., I. Shinohara, and C.-W. Jun(2018), The Level-2 orbit data of Exploration of energization and Radiation in Geospace (ERG) Arase satellite, 10.34515/DATA.ERG-12000, 2018.

406 Seki, K., K. Keika, S. Kasahara, S. Yokota, T. Hori, K. Asamura, et al.(2019). Statistical
407 properties of molecular ions in the ring current observed by the Arase (ERG) satellite. *Geophys.*
408 *Res. Lett.*, **46**, 8643–8651. doi:10.1029/2019GL084163

409 Schunk, R. W., W. J. Raitt, and P. M. Banks (1975), Effect of electric fields on the daytime high-
410 latitude E and F regions, *J. Geophys. Res.*, **80**(22), 3121–3130, doi:10.1029/JA080i022p03121.

411 Takada, M., K. Seki, Y. Ogawa, K. Keika, S. Kasahara, S. Yokota, et al. (2021). Low-altitude
412 ion upflow observed by EISCAT and its effects on supply of molecular ions in the ring current
413 detected by Arase (ERG). *J. Geophys. Res*., **126**, e2020JA028951. doi:10.1029/2020JA028951

414 Takada, M.(2023), Study of ion upflows in the low-altitude ionosphere and their effects on
415 supply of terrestrial heavy ions to the magnetosphere, doctorate in Science, University of Tokyo,
416 UTokyo Repository: http://hdl.handle.net/2261/0002008367

417 World Data Center for Geomagnetism, Kyoto, S. Imajo, A. Matsuoka, H. Toh, and T. Iyemori
418 (2022), Mid-latitude Geomagnetic Indices ASY and SYM (ASY/SYM Indices),
419 doi:10.14989/267216.

420 Wilson, G. R., and P. Craven (1999), Molecular ion upflow in the cleft ion fountain, *J. Geophys.*
421 *Res.*, **104**(A3), 4437–4446, doi:10.1029/1998JA900070.

422 Yau, A. W., T. Abe, and W. K. Peterson (2007). The Polar Wind: Recent Observations. *J. Atmos.*
423 *Solar-Terr. Phys.*, **69**, 1936–1983. doi:10.1016/j.jastp.2007.08.010

Figure 1.

(a)

H$^+$ Energy [eV/q]

count/sample

(b)

O$^+$ Energy [eV/q]

count/sample

2017 May 28	15:30	16:00	16:30	17:00	17:30	18:00	18:30	19:00	19:30
L	2.50	3.23	3.89	4.47	4.95	5.35	5.67	5.91	6.08
MLT	18.40	20.98	22.04	22.70	23.20	23.62	23.99	0.34	0.67
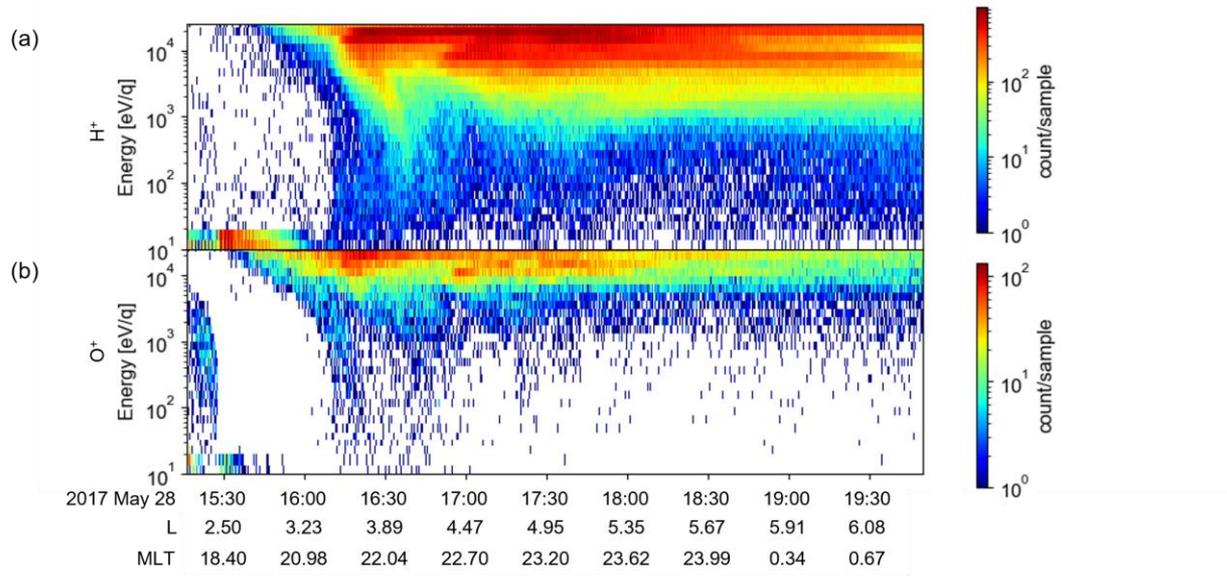
LEPi TOF (2017-05-28 15:16:14 - 2017-05-28 19:49:54)

(c)

Energy[eV/q]

N$_2^+$&NO$^+$&O$_2^+$

He^{++}

O^{++}

He$^+$

O$^+$

H$^+$

Count

(d)

Count

observed
reference

TOF[ns]
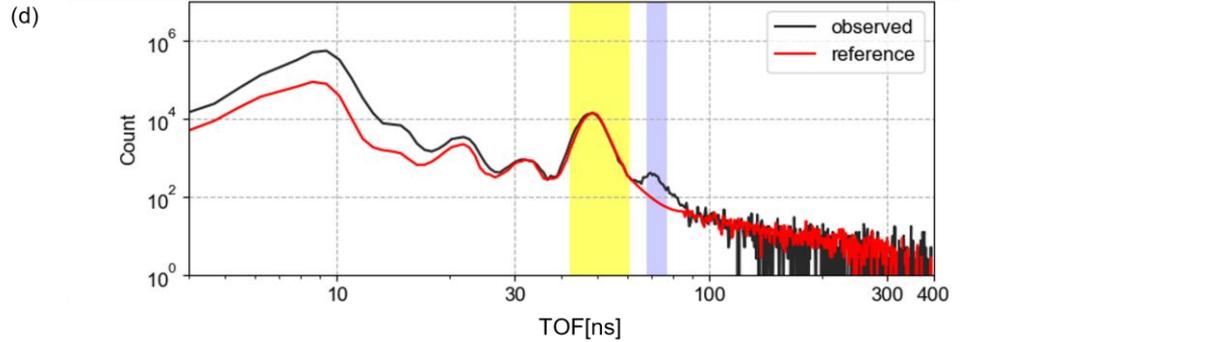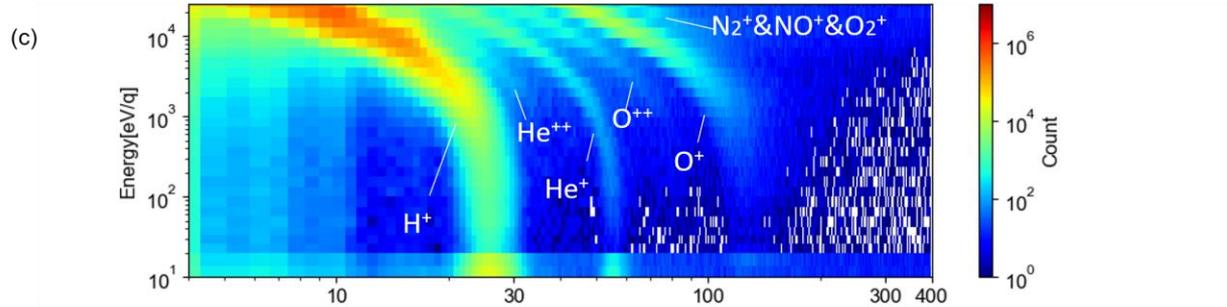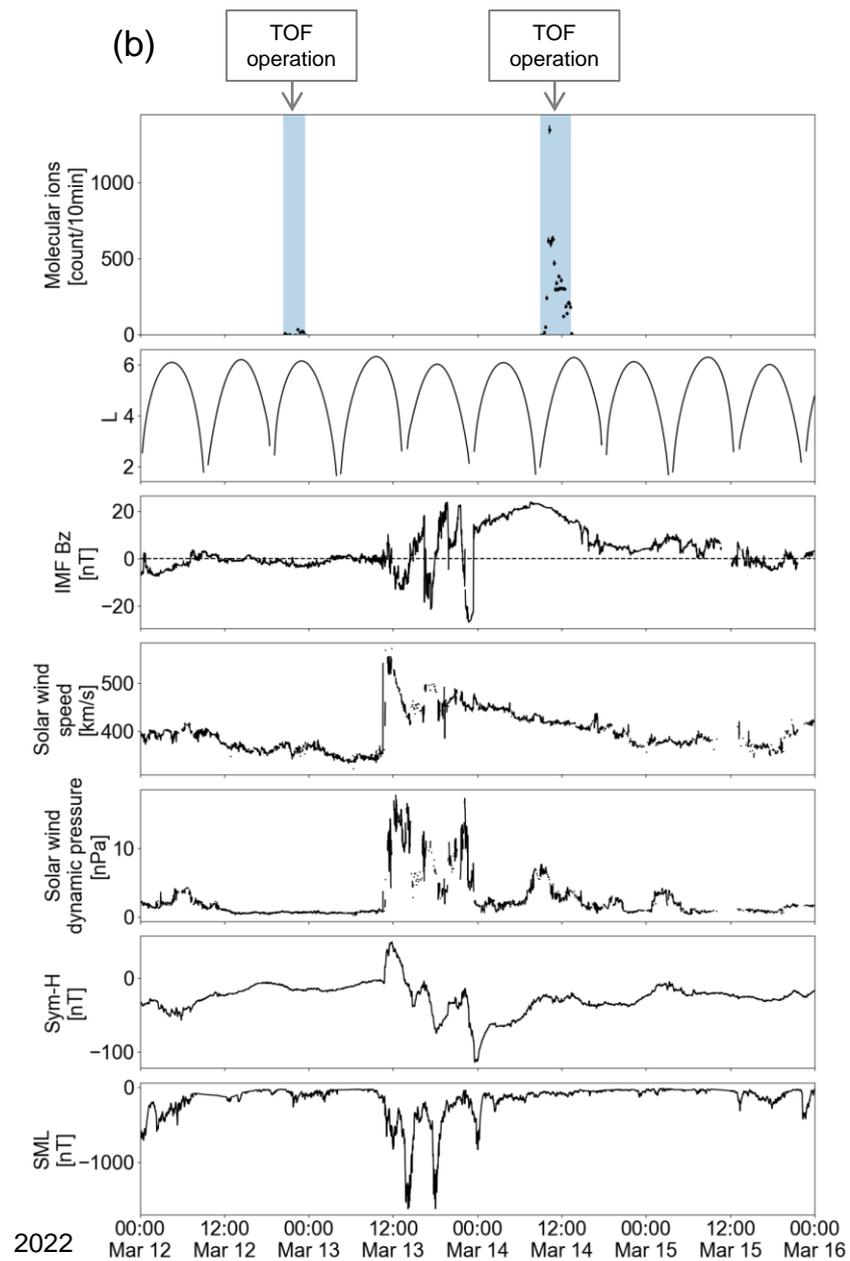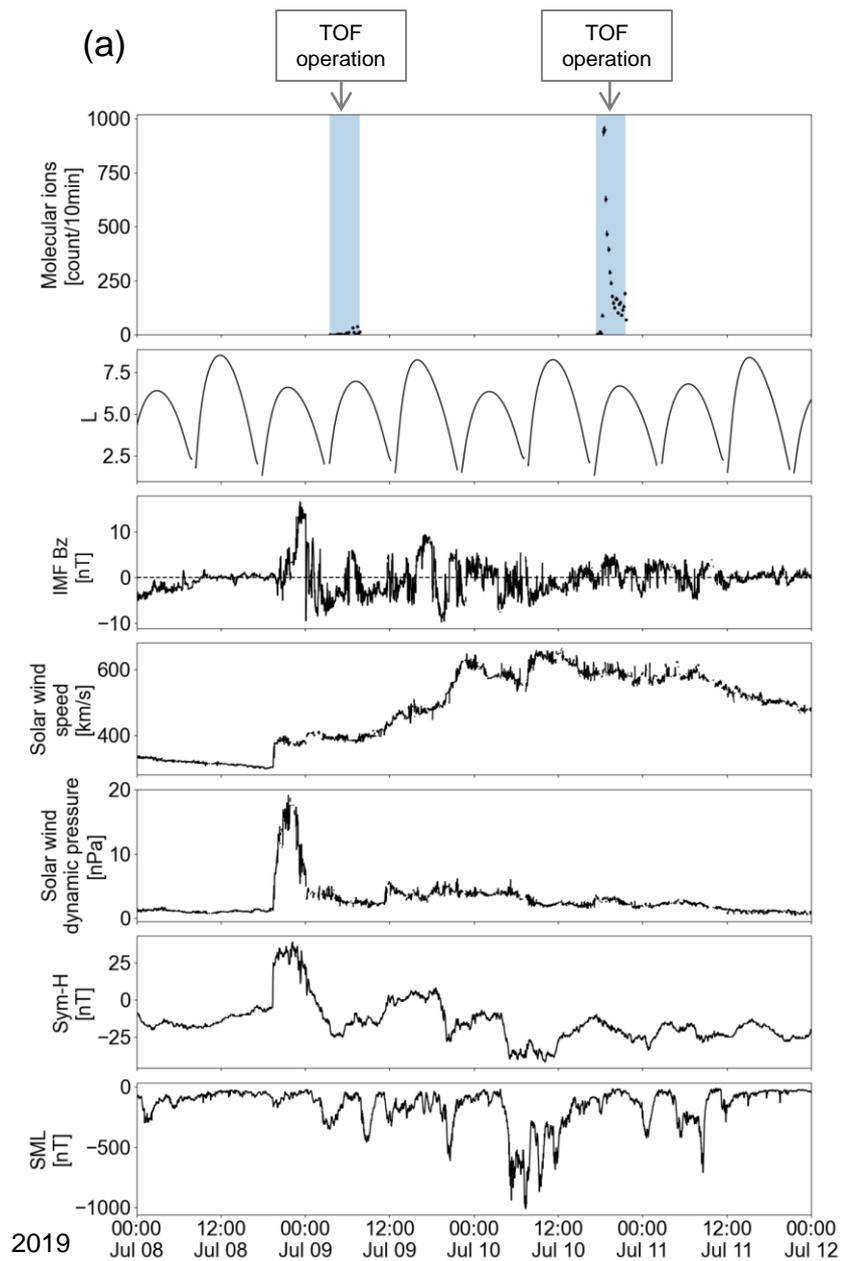
Figure 1

**Figure 2.**

Figure 2

Figure 3.

Figure 3

Figure 4.

(a)

(b)

(c)

↓ upper limit

(d)
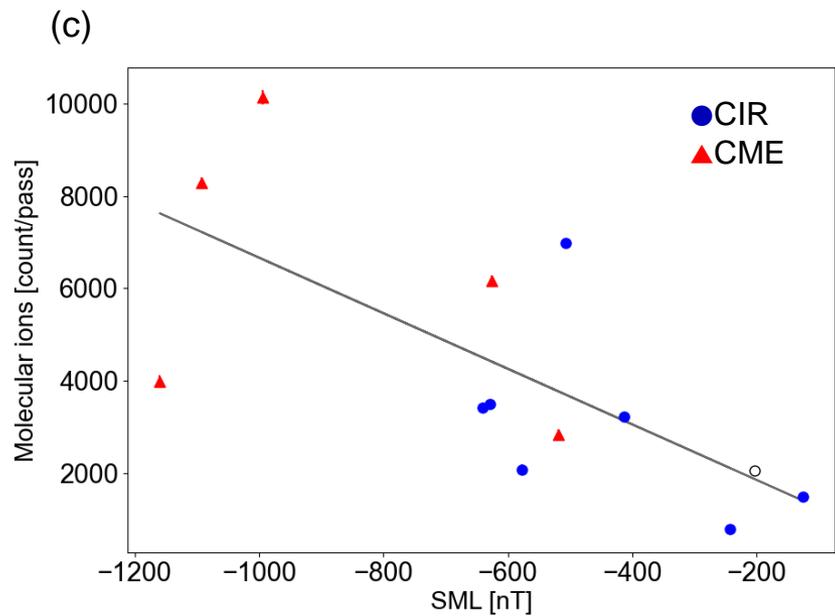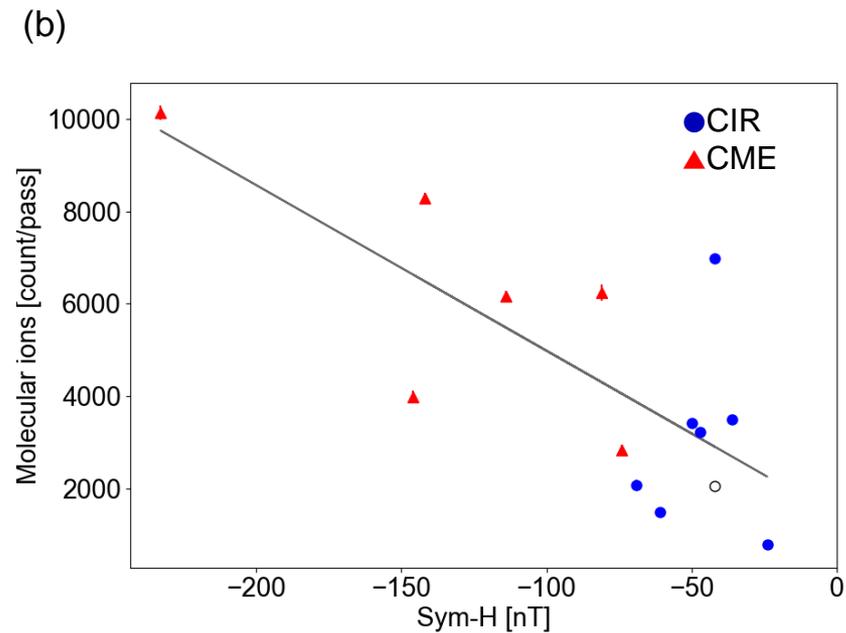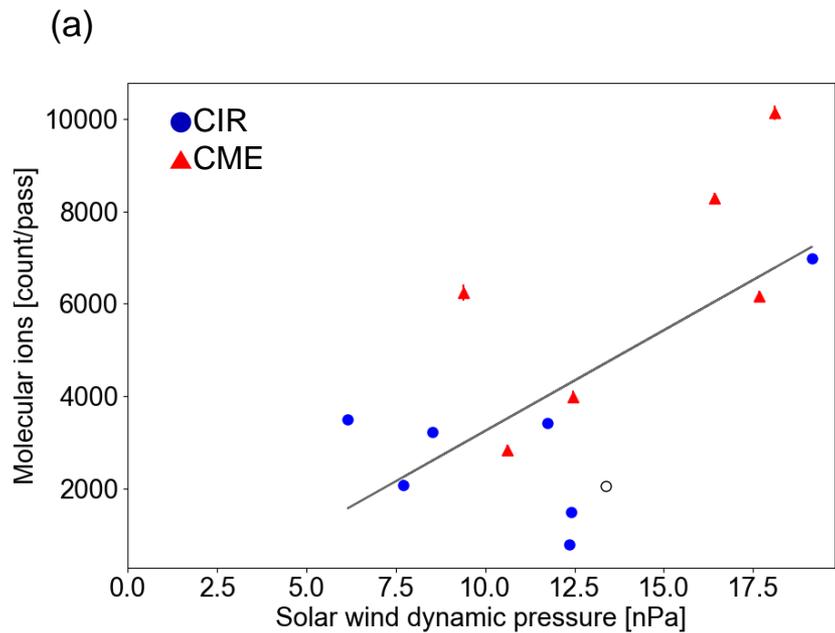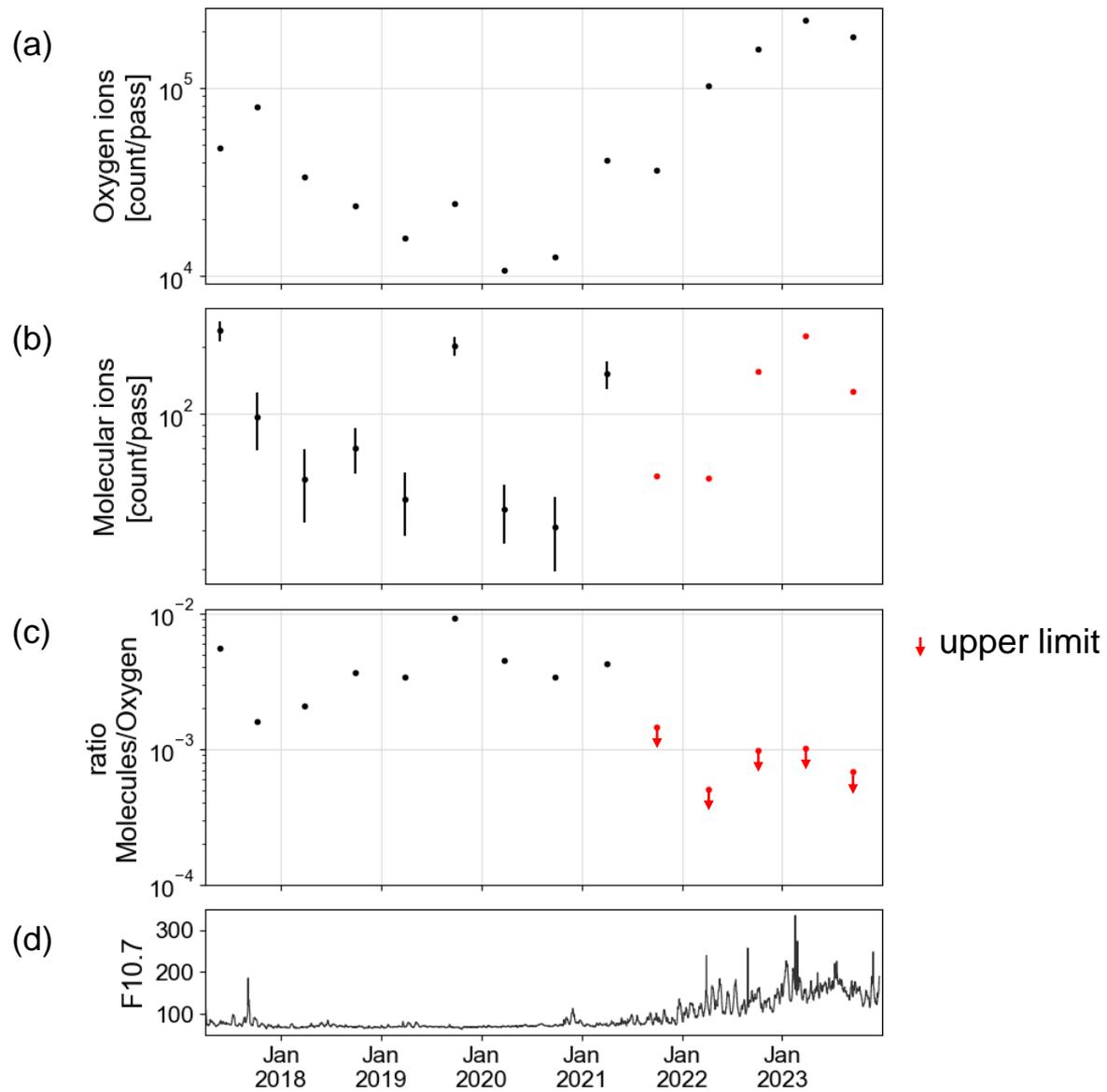
Figure 4

Figure 5.

Figure 5